A New Non-Invasive AI-Based Diagnostic System for Automated Diagnosis of Acute Renal Rejection in Kidney Transplantation: Analysis of ADC Maps Extracted from Matched 3D Iso-Regions of the Transplanted Kidney

Ibrahim Abdelhalim[1], Mohamed Abou El-Ghar[2], Amy Dwyer[3], Rosemary Ouseph[3], Sohail Contractor[4], Ayman El-Baz[1]

[1]Department of Bioengineering, University of Louisville, Louisville, KY, USA
[2]Radiology Department, Urology and Nephrology Center, Mansoura, Egypt
[3]Kidney Transplantation–Kidney Disease Center, University of Louisville, Louisville, KY, USA
[4]Department of Radiology, University of Louisville, Louisville, KY, USA

Abstract. Acute allograft rejection poses a significant challenge in kidney transplantation, the primary remedy for end-stage renal disease. Timely detection is crucial for intervention and graft preservation. A notable obstacle involves ensuring consistency across Diffusion Weighted Magnetic Resonance Imaging (DW-MRI) scanning protocols at various Tesla levels. To tackle this, we propose a novel, non-invasive framework for automated diagnosis of acute renal rejection using DW-MRI. Our method comprises several key steps: Initially, we register the segmented kidney across different scanners, aligning them from the cortex to the medulla. Afterwards, the Apparent Diffusion Coefficient (ADC) is estimated for the segmented kidney. Then, the ADC maps are partitioned into a 3D iso-surface from the cortex to the medulla using the fast-marching level sets method. Next, the Cumulative Distribution Function (CDF) of the ADC for each iso-surface is computed, and Spearman correlation is applied to these CDFs. Finally, we introduce a Transformer-based Correlations to Classes Converter (T3C) model to leverage these correlations for distinguishing between normal and acutely rejected transplants. Evaluation on a cohort of 94 subjects (40 with acute renal rejection and 54 control subjects) yields promising results, with a mean accuracy of 98.723%, a mean sensitivity of 97%, and a mean specificity of 100%, employing a leave-one-subject testing approach. These findings underscore the effectiveness and robustness of our proposed framework.

Keywords: Renal Rejection · DW-MRI · Tesla Levels · Transformer.

1 Introduction

Renal transplantation, a primary procedure in organ transplantation, is the preferred treatment for end-stage renal failure [2]. Despite progress, post-transplant

complications and increased rates of renal insufficiency pose challenges to its effectiveness [7]. Therefore, timely and accurate diagnosis and treatment are essential for the survival of transplanted kidneys. Emerging imaging techniques like Magnetic Resonance Imaging (MRI) offer noninvasive assessment of transplanted kidneys [7]. The apparent diffusion coefficient (ADC) from Diffusion-Weighted Imaging (DWI) is a reliable biomarker for renal allograft function [1]. Notably, patients with higher creatinine clearance typically have higher ADC values [6]. It has been suggested that the use of Machine Learning (ML) with high-dimensional radiomics features of MRI can provide promising performance advantages, including improved diagnostic, prognostic, and predictive accuracy, which may lead to a rapid rise in the potential use of ML in renal imaging [4, 5]. Moreover, Deep Learning (DL) techniques have garnered attention in this field. For instance, Zhi et al. [9] employed a Convolutional Neural Network (CNN) to analyze clinical and MRI data from 252 kidney-allografted patients, achieving a macro Area Under the Curve of 76.2% in distinguishing allograft conditions and predicting impaired graft function. Furthermore, Shehata et al. [8] developed a DL-based classifier using DWI, demonstrating a prediction accuracy of 97% for acute renal transplant rejection. In summary, both ML and DL models demonstrate proficiency in predicting acute renal transplant rejection. However, existing research overlooks the importance of correlations between the iso-surfaces of the kidney itself. Furthermore, significant challenges exist, including ensuring consistency across Diffusion Weighted Magnetic Resonance Imaging (DW-MRI) scanning protocols at various Tesla levels (e.g., 1.5 Tesla (T) and 3T) and addressing the shape deformation that may occur in the transplanted kidney (graft), leading to alterations in MRI diffusion signals. Additionally, models such as transformers, which hold promise for delivering more nuanced outcomes, have not been extensively utilized in this context. Moreover, there is a need for an expanded examination of different classifiers and their respective trade-offs. Also, renal transplant care is complex. Achieving a complete and accurate diagnosis during patient follow-up is an equally daunting task, fraught with challenges. The dynamic nature of graft health necessitates not just a one-time assessment but a series of exhaustive examinations using diverse MRI scanning protocols. To address these challenges, this study introduces a transformer-based framework for classifying acute renal transplant rejection using DW-MRI data obtained through various scanning protocols (specifically, 1.5T and 3T). It streamlines the difficult process of examining diverse MRI scanning protocols, thereby enhancing the accuracy of follow-up diagnoses. The framework involves several key steps. Firstly, the segmented kidney is registered with a reference image by applying a 12-degree-of-freedom affine-based registration, followed by a non-rigid 3D B-spline transformation [3] to ensure alignment of the main regions within the kidney (cortex, medulla, renal pyramids, renal pelvis, etc.). In the next step, the ADC maps of the segmented kidney are calculated. After that, iso-surfaces are generated from these maps. Then, we compute the Cumulative Distribution Function (CDF) for each iso-surface. The Spearman correlation algorithm is then applied to these CDFs corresponding to iso-surfaces. Finally, a transformer-based

model is employed to leverage these correlations to distinguish between normal and acutely rejected transplants. To sum up, our contributions are twofold:

- We introduce a novel transformer-based framework for classifying acute renal transplant rejection using DW-MRI data obtained through various scanning protocols, which is a new approach that accounts for variations in scanner types and mitigates potential effects on MRI signals based on the correlations.
- We propose a Transformer-based Correlations to Classes Converter (T3C) model to leverage the correlations of the CDFs to distinguish between normal and acutely rejected transplants, highlighting the effectiveness and versatility of the transformer model in this context.

2 Methodology

A transformer-based framework is introduced to predict acute renal transplant rejection using diverse DW-MRI scanning protocols (see Figure 1). The framework begins with preprocessing, which yields segmented ADC maps. Then, isosurfaces are generated to represent distinct kidney regions. Afterwards, the T3C model leverages the correlations of CDFs which correspond to these regions for a comprehensive prediction of kidney states.

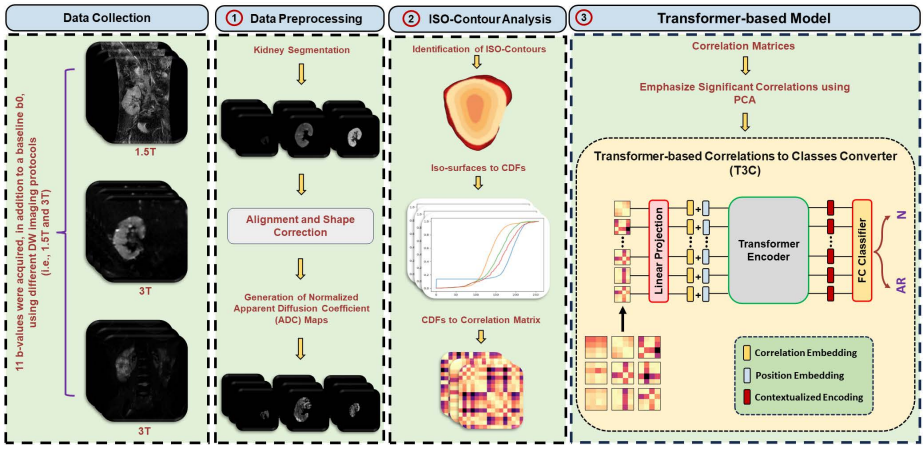

Fig. 1. An overview of the proposed framework employs data from various DW-MRI scanning protocols to predict both normal and acute rejection.

2.1 Preprocessing

As depicted in Figure 1, this step involves subjecting the DW-MRI scans to segmentation to extract kidney using in-house software. A common challenge

in DW-MRIs is the shape deformation that can lead to the alteration of MRI diffusion signals. The geometric shapes of anatomical structures can also affect the prediction accuracy. Therefore, the segmented kidneys undergo processing to align them and eliminate their deformation in intra-patient scenarios, such as due to breathing and/or heart beating, and to account for the kidney's variability due to inter-patient anatomical differences. Specifically, one of the 3D images is chosen as a reference image and all other 3D images are aligned to it by applying a 12-degree-of-freedom affine-based registration. To further correct the shape deformation, a non-rigid 3D B-spline transformation [3] is applied (see Figure 2). Afterwards, the registered kidneys are transformed to yield their corresponding ADC maps. These ADC maps are then used as inputs for the next step.

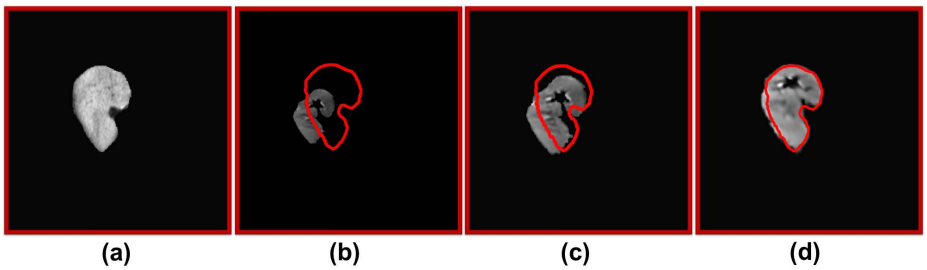

Fig. 2. This figure illustrates a cross-section of 3D images through the registration process. (a) displays the reference image, while (b) presents the moving image. (c) and (d) show the outcomes following a 12-degree-of-freedom affine-based registration and the result obtained from a non-rigid 3D B-spline transformation, respectively.

2.2 ISO-surface Analysis

This study aims to develop a non-invasive method for identifying potential abnormalities indicative of renal rejection. To achieve this, we leverage correlations of CDFs which correspond to iso-surfaces of the kidney. Since the correlation measures the strength and direction of a linear relationship between two variables (in this case, the CDFs of iso-surfaces), we focus on the relationship patterns between distributions of different kidney regions using correlation rather than analyzing the raw imaging data directly. This approach mitigates the impact of scanner-induced variations on the raw imaging data values, which can be influenced by the specific characteristics of the scanner. To identify iso-surfaces, we employ a fast marching algorithm. Furthermore, the Spearman correlation is used for calculating correlations. The rationale behind using the Spearman correlation algorithm is its ability to assess monotonic relationships, determining whether there is a linear pattern or not between iso-surfaces. Upon visual inspection of Figure 3, which displays the correlations 3D iso-surfaces for two patients (a) and (b), it is evident that the acutely rejected kidney, as shown in

(b), exhibits variations in correlation when compared to the normal kidney, as illustrated in (a). These variations suggest potential abnormalities within these regions, indicative of renal rejection.

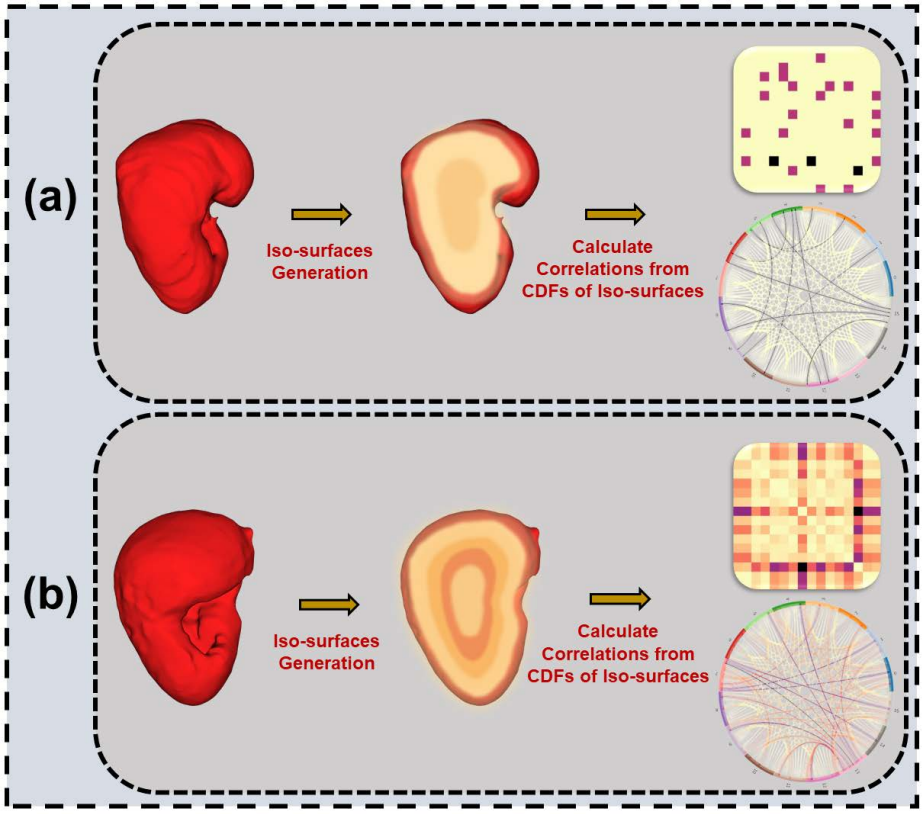

Fig. 3. The process flow from acquiring the iso-surfaces to calculating the corresponding correlations is presented. (a) represents a normal case, while (b) shows an acute rejection case where the correlations experience variations, indicative of renal rejection.

2.3 Transformer-based Correlations to Classes Converter (T3C)

In the final stage, the correlations derived from the previous step undergo transformation via Principal Component Analysis (PCA). This is done to reduce the dimensionality of the obtained correlations, discarding those of lesser significance while preserving the essential ones (see Figures 1 and 4). This procedure aids in the development of a robust model that can accurately predict the status of transplanted kidneys, differentiating between normal function and instances of acute rejection. To achieve this, we have designed a T3C model

that learns to map correlations to class scores. Specifically, a correlation tensor $x \in \mathbb{R}^{N \times R \times C}$ is defined, where N represents the number of b-values for each patient, R is the number of rows, and C is the number of columns. This tensor is reshaped and linearly transformed to produce a sequence of correlation embeddings $x = [e_1, ..., e_N] \in \mathbb{R}^{N \times L}$, where $e \in \mathbb{R}^L$. To maintain positional information, learnable position embeddings $p = [p_1, ..., p_N] \in \mathbb{R}^{N \times L}$ are added to the correlation embeddings, resulting in the input sequence of tokens $z = x + p$. The T3C model's transformer encoder, composed of H layers, processes the input sequences z, generating contextualized encodings $z_H \in \mathbb{R}^{N \times L}$. Each transformer layer consists of a multi-headed self-attention (MSA) block followed by a point-wise MLP block, with layer normalization (LN) applied before and residual connections added after each block:

$$a_{i-1} = \text{MSA}(\text{LN}(z_{i-1})) + z_{i-1},$$
$$z_i = \text{MLP}(\text{LN}(a_{i-1})) + a_{i-1},$$

where $i \in \{1, ..., H\}$. The self-attention mechanism computes queries $\mathbf{Q} \in \mathbb{R}^{N \times d}$, keys $\mathbf{K} \in \mathbb{R}^{N \times d}$, and values $\mathbf{V} \in \mathbb{R}^{N \times d}$ via three point-wise linear layers and then computes self-attention as:

$$\mathbf{MSA}(\mathbf{Q}, \mathbf{K}, \mathbf{V}) = \text{softmax}\left(\frac{\mathbf{Q}\mathbf{K}^T}{\sqrt{d}}\right)\mathbf{V}$$

The transformer encoder maps the input sequences to a contextualized encoding sequence $z_H = [z_{H,1}, ..., z_{H,N}]$ that contains rich salient information. Subsequently, z_H is utilized by a Fully Connected (FC) classifier to obtain class scores corresponding to normal and acute rejection. Please refer to Figure 1 for a better understanding of the developed T3C model.

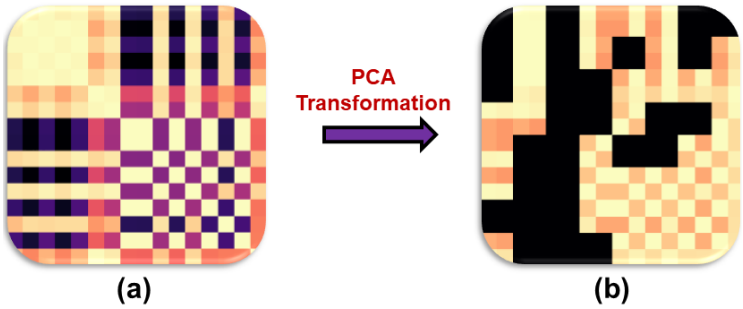

Fig. 4. The procedure involves applying PCA to the correlations. (a) depicts the original Spearman correlation matrix, while (b) illustrates the matrix after retaining significant correlations and discarding insignificant ones.

3 Experiments and Results

Dataset. This study's dataset includes DW-MRI scans from 94 patients. Of these, 34 were obtained using a 1.5T SIGNA Horizon scanner, adhering to specific parameters for coronal DW-MR images. The scans included 11 b-values sequences and baseline b0 scans, capturing blood perfusion and water diffusion effects. Each sequence used a single DW-MRI direction with equal gradient amplitudes. Furthermore, 60 DW-MRI scans were performed using a 3T scanner, following similar protocols with minor adjustments due to different scanner models. Each scan also included 11 b-values and the baseline b0.

Setting. We utilize an Adam optimizer with a learning rate of 0.001 over 100 epochs. Leave-one-out cross-validation is employed for evaluating the models, and the reported results represent the mean of ten runs. Additionally, L2 loss is utilized for training the model. The implementation was carried out using PyTorch on a single NVIDIA Quadro P4000 GPU with 8GB of memory.

Results and Analysis. We conducted two main experiments: the first used classical ML classifiers to categorize correlations, while the second utilized the proposed transformer-based model. As shown in Table 1, among the ML classifiers, Random Forest (RF) achieved the highest mean Accuracy (ACC) of 51.915%, mean Specificity (SPE) of 70.370%, and mean Area Under the Curve (AUC) of 48.685%. Decision Tree (DT) attained the highest mean Sensitivity (SEN) of 42.250% compared to Multi-Layer Perceptron (MLP) and Gradient Boosting (GB). However, the T3C model outperformed all others, boasting a mean ACC of 98.723%, mean SEN of 97%, mean SPE of 100%, and mean AUC of 98.5%, surpassing RF, DT, MLP, and GB. To further validate our model's superiority, we conducted a Mann–Whitney statistical test, revealing significant statistical superiority with a p-value less than 0.001 compared to other classifiers. Our findings have profound implications for clinical practice, as accurate prediction of normalcy or acute rejection in transplanted kidneys is crucial for effective treatment planning and monitoring. However, it is important to acknowledge the limitations of our approach, notably the relatively small cohort of only 94 patients

Table 1. A comparison of the classification results between the T3C model and classical ML classifiers is presented. The mean±standard deviation, expressed in percentage, along with the statistical significance, are reported. Notably, the p-value for our model, when compared to other classifiers, was found to be less than 0.001, indicating a high level of statistical significance.

Classifier	ACC	SEN	SPE	AUC	Mann–Whitney
RF	51.915 ± 3.184	27.000 ± 7.399	70.370 ± 5.617	48.685 ± 3.340	1.62×10^{-4}
DT	41.596 ± 3.478	42.250 ± 4.931	41.111 ± 4.040	41.681 ± 3.538	1.62×10^{-4}
MLP	44.787 ± 1.809	32.250 ± 2.839	54.074 ± 2.845	43.162 ± 1.777	1.46×10^{-4}
GB	47.553 ± 1.069	28.750 ± 1.250	61.481 ± 1.814	45.116 ± 0.991	1.33×10^{-4}
T3C	$\mathbf{98.723 \pm 1.241}$	$\mathbf{97.000 \pm 2.915}$	$\mathbf{100.000 \pm 0}$	$\mathbf{98.500 \pm 1.458}$	–

4 Conclusions and Future Work

This research paper introduces a novel framework for predicting both normal kidney function and instances of acute rejection. The framework leverages diverse DW-MRI datasets obtained through various scanning protocols, specifically, 1.5T and 3T. This approach effectively addresses the primary challenge of creating a system robust to variations in DW-MRI protocol across different scanners. The framework's remarkable sensitivity and specificity results establish its potential as a significant tool for treatment planning and monitoring patient responses to kidney transplants. Future work plans to broaden the study with larger cohorts, investigate additional imaging modalities, explore the impact of different correlation algorithms, develop an end-to-end detection framework, and evaluate the integration of clinical biomarkers such as creatinine clearance and serum creatinine.

Disclosure of Interests. The authors have no competing interests.

References

1. Baliyan, V., Das, C.J., Sharma, R., Gupta, A.K.: Diffusion weighted imaging: technique and applications. World journal of radiology **8**(9), 785 (2016)
2. Cavallo, M., Sepe, V., Conte, F., Abelli, M., Ticozzelli, E., Bottazzi, A., Geraci, P.: Cost-effectiveness of kidney transplantation from dcd in italy. In: Transplantation proceedings. vol. 46, pp. 3289–3296. Elsevier (2014)
3. Glocker, B., Komodakis, N., Paragios, N., Navab, N.: Non-rigid registration using discrete mrfs: Application to thoracic ct images. In: Workshop Evaluation of Methods for Pulmonary Image Registration in conjunction with Medical Image Computing and Computer-Assisted Intervention. Springer International Publishing (2010)
4. Kline, T.L., Korfiatis, P., Edwards, M.E., Bae, K.T., Yu, A., Chapman, A.B., Mrug, M., Grantham, J.J., Landsittel, D., Bennett, W.M., et al.: Image texture features predict renal function decline in patients with autosomal dominant polycystic kidney disease. Kidney international **92**(5), 1206–1216 (2017)
5. Lee, H.C., Yoon, H.K., Nam, K., Cho, Y.J., Kim, T.K., Kim, W.H., Bahk, J.H.: Derivation and validation of machine learning approaches to predict acute kidney injury after cardiac surgery. Journal of clinical medicine **7**(10), 322 (2018)
6. Palmucci, S., Mauro, L., Failla, G., Foti, P., Milone, P., Sinagra, N., Zerbo, D., Veroux, P., Ettorre, G., Veroux, M.: Magnetic resonance with diffusion-weighted imaging in the evaluation of transplanted kidneys: updating results in 35 patients. In: Transplantation proceedings. vol. 44, pp. 1884–1888. Elsevier (2012)
7. Sharfuddin, A.: Renal relevant radiology: imaging in kidney transplantation. Clinical journal of the American Society of Nephrology: CJASN **9**(2), 416 (2014)
8. Shehata, M., Khalifa, F., Soliman, A., Ghazal, M., Taher, F., Abou El-Ghar, M., Dwyer, A.C., Gimel'farb, G., Keynton, R.S., El-Baz, A.: Computer-aided diagnostic system for early detection of acute renal transplant rejection using diffusion-weighted mri. IEEE Transactions on Biomedical Engineering **66**(2), 539–552 (2018)
9. Zhi, R., Zhang, X.D., Hou, Y., Jiang, K.W., Li, Q., Zhang, J., Zhang, Y.D.: Rtnet: a deep hybrid neural network for the identification of acute rejection and chronic allograft nephropathy after renal transplantation using multiparametric mri. Nephrology Dialysis Transplantation **37**(12), 2581–2590 (2022)